BJP British Journal of Pharmacology

DOI:10.1111/bph.12002
www.brjpharmacol.org

RESEARCH PAPER

Mechanisms of zolpidem-induced long QT syndrome: acute inhibition of recombinant hERG K^+ channels and action potential prolongation in human cardiomyocytes derived from induced pluripotent stem cells

J Jehle[1], E Ficker[2], X Wan[2], I Deschenes[2], J Kisselbach[1], F Wiedmann[1], I Staudacher[1], C Schmidt[1], PA Schweizer[1], R Becker[1], HA Katus[1] and D Thomas[1]

[1]*Department of Cardiology, Medical University Hospital, Heidelberg, Heidelberg, Germany, and* [2]*Rammelkamp Center, MetroHealth Campus, Case Western Reserve University, Cleveland, OH, USA*

Correspondence
Dierk Thomas, Department of Cardiology, University of Heidelberg, Im Neuenheimer Feld 410, D-69120 Heidelberg, Germany. E-mail: dierk.thomas@med.uni-heidelberg.de

Keywords
action potential; hERG K^+ channel; long QT syndrome; torsade de pointes; zolpidem

Received
16 July 2012
Revised
9 September 2012
Accepted
23 September 2012

BACKGROUND AND PURPOSE

Zolpidem, a short-acting hypnotic drug prescribed to treat insomnia, has been clinically associated with acquired long QT syndrome (LQTS) and torsade de pointes (TdP) tachyarrhythmia. LQTS is primarily attributed to reduction of cardiac human ether-a-go-go-related gene (hERG)/I_{Kr} currents. We hypothesized that zolpidem prolongs the cardiac action potential through inhibition of hERG K^+ channels.

EXPERIMENTAL APPROACH

Two-electrode voltage clamp and whole-cell patch clamp electrophysiology was used to record hERG currents from *Xenopus* oocytes and from HEK 293 cells. In addition, hERG protein trafficking was evaluated in HEK 293 cells by Western blot analysis, and action potential duration (APD) was assessed in human-induced pluripotent stem cell (hiPSC)-derived cardiomyocytes.

KEY RESULTS

Zolpidem caused acute hERG channel blockade in oocytes (IC_{50} = 61.5 μM) and in HEK 293 cells (IC_{50} = 65.5 μM). Mutation of residues Y652 and F656 attenuated hERG inhibition, suggesting drug binding to a receptor site inside the channel pore. Channels were blocked in open and inactivated states in a voltage- and frequency-independent manner. Zolpidem accelerated hERG channel inactivation but did not affect *I–V* relationships of steady-state activation and inactivation. In contrast to the majority of hERG inhibitors, hERG cell surface trafficking was not impaired by zolpidem. Finally, acute zolpidem exposure resulted in APD prolongation in hiPSC-derived cardiomyocytes.

CONCLUSIONS AND IMPLICATIONS

Zolpidem inhibits cardiac hERG K^+ channels. Despite a relatively low affinity of zolpidem to hERG channels, APD prolongation may lead to acquired LQTS and TdP in cases of reduced repolarization reserve or zolpidem overdose.

Abbreviations

APD, action potential duration; DMSO, dimethyl sulfoxide; hERG, human ether-a-go-go-related gene; hiPSC, human-induced pluripotent stem cell; LQTS, long QT syndrome; TdP, torsade de pointes; WT, wild type

Introduction

Zolpidem is a non-benzodiazepine hypnotic drug that is commonly prescribed to initiate sleep in patients suffering from insomnia (Nicholson and Pascoe, 1986; Dündar *et al.*, 2004; Hausken *et al.*, 2009). Cardiac safety concerns have been raised by a case of long QT syndrome (LQTS) complicated by torsade de pointes (TdP) tachyarrhythmia in a patient simultaneously receiving zolpidem and amiodarone (Letsas *et al.*, 2006). Acquired LQTS is a potentially lethal cardiac electrical disorder that is commonly caused by drug-induced reduction of the repolarizing I_{Kr} current (Viskin, 1999; Thomas *et al.*, 2006). The human ether-a-go-go-related gene (hERG, KCNH2 or Kv11.1) encodes the ion channel α subunit underlying I_{Kr} (Sanguinetti and Tristani-Firouzi, 2006). At the molecular level, I_{Kr} reduction may be caused by at least three different mechanisms: (i) acute inhibition of hERG channels, (ii) acute internalization of hERG surface protein and (iii) chronic disruption of hERG protein forward trafficking (Lacerda *et al.*, 2001; Ficker *et al.*, 2004; Zitron *et al.*, 2004; Thomas *et al.*, 2004a; 2006; Rajamani *et al.*, 2006; Guo *et al.*, 2007; Takemasa *et al.*, 2007; Wang *et al.*, 2007; Van der Heyden *et al.*, 2008; Obers *et al.*, 2010; Staudacher *et al.*, 2010; 2011a; Dennis *et al.*, 2011). In addition to the heart, hERG potassium channels are expressed in tumour cells where they are involved in the regulation of cell proliferation and apoptosis (Bianchi *et al.*, 1998; Cherubini *et al.*, 2000; Smith *et al.*, 2002; Wang *et al.*, 2002). Recently, inhibition of cardiac hERG channels has been revealed to promote apoptosis, suggesting a novel mechanism of cardiotoxicity (Thomas *et al.*, 2008; Gong *et al.*, 2010; Obers *et al.*, 2010; Staudacher *et al.*, 2011a). In contrast to electrophysiological effects of hERG current reduction leading to LQTS, hERG-associated apoptosis may contribute to cardiomyocyte loss and heart failure.

hERG-linked adverse effects represent a significant cardiovascular liability of clinical and developmental drugs. A comprehensive understanding of underlying molecular mechanisms is required to optimize preclinical screening procedures and to reduce potentially life-threatening drug side effects. To date, there are no reports on hERG-related effects of zolpidem. Consequently, we designed this study to investigate zolpidem effects on hERG currents, hERG protein surface expression, cardiac action potential duration and hERG-associated apoptosis. First, acute electrophysiological effects of zolpidem on recombinant hERG channels expressed in *Xenopus laevis* oocytes and in HEK 293 cells were analysed in detail. Second, prolongation of cardiac action potentials in human cardiomyocytes derived from induced pluripotent stem cells was demonstrated. Next, Western blot analysis was performed to reveal a lack of drug effects on hERG protein surface expression (HEK 293 cells). Finally, zolpidem did not trigger apoptosis in HL-1 cardiac myocytes.

Methods

Molecular biology

Drug target nomenclature conforms with British Journal of Pharmacology's *Guide to Receptors and Channels* (Alexander *et al.*, 2011). *In vitro* transcription and oocyte injection were performed as published previously (Kiehn *et al.*, 1999). Y652A and F656A point mutations in hERG wild type (WT; GenBank accession no. NM_000238) were introduced using a QuikChange site-directed mutagenesis kit (Stratagene, La Jolla, CA) and synthetic mutant oligonucleotide primers. DNA sequences were cloned into the pSP64 vector and linearized using Eco*RI* (Roche Diagnostics, Mannheim, Germany). All cDNA constructs were confirmed by DNA sequencing. Subsequently, cRNAs were transcribed using SP6 RNA polymerase and the mMessage mMachine kit (Ambion, Austin, TX). Transcripts were quantified photometrically and by comparison with control samples separated by agarose gel electrophoresis.

Oocyte preparation

All studies involving animals are reported in accordance with the ARRIVE guidelines for reporting experiments involving animals (McGrath *et al.*, 2010). The investigation conforms to the Directive 2010/63/EU of the European Parliament. Approval was granted by the local Animal Welfare Committee (reference number A-38/11). All experiments have been carried out in accordance with the United States National Institutes of Health Guide for the Care and Use of Laboratory Animals (NIH Publication no. 85–23, revised 1996) as reported earlier (Gierten *et al.*, 2008; Staudacher *et al.*, 2011b; Seyler *et al.*, 2012). Briefly, oocytes were isolated from *X. laevis* ovarian lobes after surgical extirpation during tricaine anaesthesia (1 g L^{-1}; pH 7.5). Oocyte collection was alternated between left and right ovaries, and a maximum of three surgeries were performed on one individual frog. After the final collection of oocytes, anaesthetized frogs were killed by decerebration and pithing. cRNA (~800 ng μL^{-1}; 46–92 nL per oocyte) was injected into stage V–VI defolliculated *Xenopus* oocytes.

Cell culture

cDNA encoding the hERG WT potassium channel cloned in pCDNA3 was stably transfected into the HEK 293 cell line as described (Thomas *et al.*, 2001; Ficker *et al.*, 2003; 2004). Cells were cultured in DMEM (Gibco BRL, Rockville, IL) supplemented with 10% FBS, 2 mM L-glutamine, 100 U mL^{-1} penicillin G sodium, 100 μg mL^{-1} streptomycin sulphate and 500 μg mL^{-1} geneticin (G418; all from Gibco BRL) in an atmosphere of 95% humidified air and 5% CO_2 at 37°C. Cells were passaged regularly and subcultured prior to treatment. Drugs were added prior to Western blot analyses as indicated.

Human-induced pluripotent stem cell (hiPSC)-derived cardiomyocytes (iCell Cardiomyocytes; Cellular Dynamics

International, Madison, WI) were cultured in iCell Cardiomyocytes Maintenance Medium (Cellular Dynamics International) in an atmosphere of 93% humidified air and 7% CO_2 at 37°C. For electrophysiological recordings, 20 000–40 000 cardiomyocytes were plated on glass coverslips coated with 0.1% gelatin as described (Ma *et al.*, 2011).

HL-1 cells, a cardiac cell line derived from the AT-1 mouse atrial myocyte tumour lineage, were kindly provided by Dr William Claycomb (New Orleans, LA) (Claycomb *et al.*, 1998). Cells were cultured and maintained in Claycomb medium, supplemented with 10% FBS, 1% norepinephrine (Sigma-Aldrich, Steinheim, Germany), 2 mM L-glutamine, 100 U mL^{-1} penicillin G sodium and 100 μg mL^{-1} streptomycin sulphate (G418; Gibco BRL) as described (Claycomb *et al.*, 1998; Lugenbiel *et al.*, 2012; Trappe *et al.*, 2012). Drug treatment was performed when cells were 80% confluent.

Electrophysiology

Two-electrode voltage clamp measurements and whole cell patch clamp recordings were performed as reported earlier (Thomas *et al.*, 1999; 2001; Soucek *et al.*, 2012). Voltage clamp electrodes had tip resistances of 1–5 MΩ and were filled with the following solution (in mM) 3 KCl, 102 NaCl, 1.5 $CaCl_2$, 2 $MgCl_2$ and 10 HEPES (pH adjusted to 7.4 with NaOH): Voltage clamp measurements of *Xenopus* oocytes were carried out with an Oocyte Clamp amplifier (Warner Instruments, Hamden, CT) in a solution containing (in mM): 5 KCl, 100 NaCl, 1.5 $CaCl_2$, 2 $MgCl_2$ and 10 HEPES (pH adjusted to 7.4 with NaOH). Data were sampled at 2 kHz and filtered at 1 kHz. Recordings were performed under constant superfusion at room temperature 1–4 days after RNA injection.

Current recordings from HEK 293 cells were carried out using the whole-cell patch clamp configuration as reported (Thomas *et al.*, 2001). To analyse current densities, membrane capacitance was measured using the analogue compensation circuit of the patch clamp amplifier. Patch clamp electrodes were filled with the following solution (in mM): 100 K-aspartate, 20 KCl, 2.0 $MgCl_2$, 1 $CaCl_2$, 10 EGTA, 10 HEPES (pH adjusted to 7.2 with KOH). The external solution contained (in mM): 140 NaCl, 5.0 KCl, 1.0 $MgCl_2$, 1.8 $CaCl_2$, 10 HEPES, 10 glucose (pH adjusted to 7.4 with NaOH). To study long-term drug effects on hERG currents, zolpidem was added overnight prior to recordings as indicated. hERG current recordings were carried out at room temperature (20–22 °C), and no leak subtraction was done during the experiments.

Ventricular-like action potentials were recorded from human cardiomyocytes derived from induced pluripotent stem cells. The perforated patch technique was used to preserve the intracellular milieu of the intact cardiomyocyte. Patch pipettes were filled with (in mM): 120 K-aspartate, 20 KCl, 10 NaCl, 2.0 $MgCl_2$, 5 HEPES (pH adjusted to 7.3 with KOH), supplemented with 240 μg mL^{-1} amphotericin-B (Sigma-Aldrich). The extracellular solution was Tyrode's solution (137 mM NaCl, 5.4 mM KCl, 2 mM $CaCl_2$, 1 mM $MgSO_4$, 10 mM glucose and 10 mM HEPES, pH 7.3). Following seal formation, access resistance was continuously monitored. Experimental protocols were initiated after the access resistance dropped below 40 MΩ. Action potentials were elicited in current clamp mode at a stimulation frequency of 1 Hz and recorded at 35°C.

Macroscopic currents and action potentials were measured using pCLAMP (Molecular Devices, Sunnyvale, CA) and Origin (OriginLab, Northampton, MA) software for data acquisition and analysis.

Western blot analysis

Immunodetection of hERG protein was performed by SDS gel electrophoresis and Western blotting. HEK-hERG cells were solubilized for 1 h at 4°C in lysis buffer containing 1% Triton X-100 and 'Complete' protease inhibitors (Roche Diagnostics, Indianapolis, IN). Protein concentrations were determined with the BCA method (Pierce, Rockford, IL). Proteins were then separated on SDS polyacrylamide gels, transferred to PVDF membranes and detected using rabbit anti-hERG polyclonal antibody (hERG 519; Ficker *et al.*, 2003) and appropriate HRP-conjugated secondary antibodies. ECL Plus reagent (GE Healthcare, Piscataway, NJ) was used for signal development. For quantitative analyses, chemiluminescence signals were captured directly on a Kodak Imaging Station 4000R (Ficker *et al.*, 2003).

TUNEL staining

Apoptosis was detected by TUNEL staining. Following exposure to zolpidem, cells grown in 24-well tissue culture dishes were fixed and TUNEL reaction mixture (Roche Applied Science, Mannheim, Germany) was added to the sections according to the manufacturer's instructions, followed by incubation at 37°C for 60 min. TUNEL reagent was then removed, slides were rinsed with PBS and TUNEL-positive cells were evaluated using a fluorescence microscope (IX 50; Olympus, Hamburg, Germany).

Solutions and drugs

Zolpidem (Sigma-Aldrich) was prepared as 100 mM stock solution in dimethyl sulfoxide (DMSO) and stored at –20°C. Amiodarone (Sigma-Aldrich) was dissolved in ethanol to a stock solution of 10 mM and stored at 4°C. hERG tail currents (recorded as described in Figure 1A) were not affected by application of DMSO at its maximum concentration [0.3% (v/v) DMSO] ($I_{control}/I_{DMSO,30\ min} = 0.96 \pm 0.01$; $n = 5$; $P = 0.54$). On the day of experiments, aliquots of the stock solution were diluted to the desired concentrations with bath solution or culture media respectively.

Data analysis

PCLAMP (Axon Instruments, Foster City, CA), Origin 6 (OriginLab) and Excel (Microsoft, Redmond, WA) software were used for data acquisition and analysis. Concentration–response relationships for drug-induced block were calculated using sigmoidal fits (Origin 6). Activation and inactivation curves were fit with a single-power Boltzmann distribution of the form $I = I_{max}/[1 + e^{(V1/2-V)/k}]$, where V is the test pulse potential, $V_{1/2}$ is the half-maximal activation/inactivation potential and k is the slope of the activation curve.

Statistics

Data are expressed as mean ± SEM. We used paired and unpaired Student's *t*-tests (two-tailed tests) to compare the statistical significance of the results where appropriate. $P < 0.05$ was considered statistically significant. Multiple com-

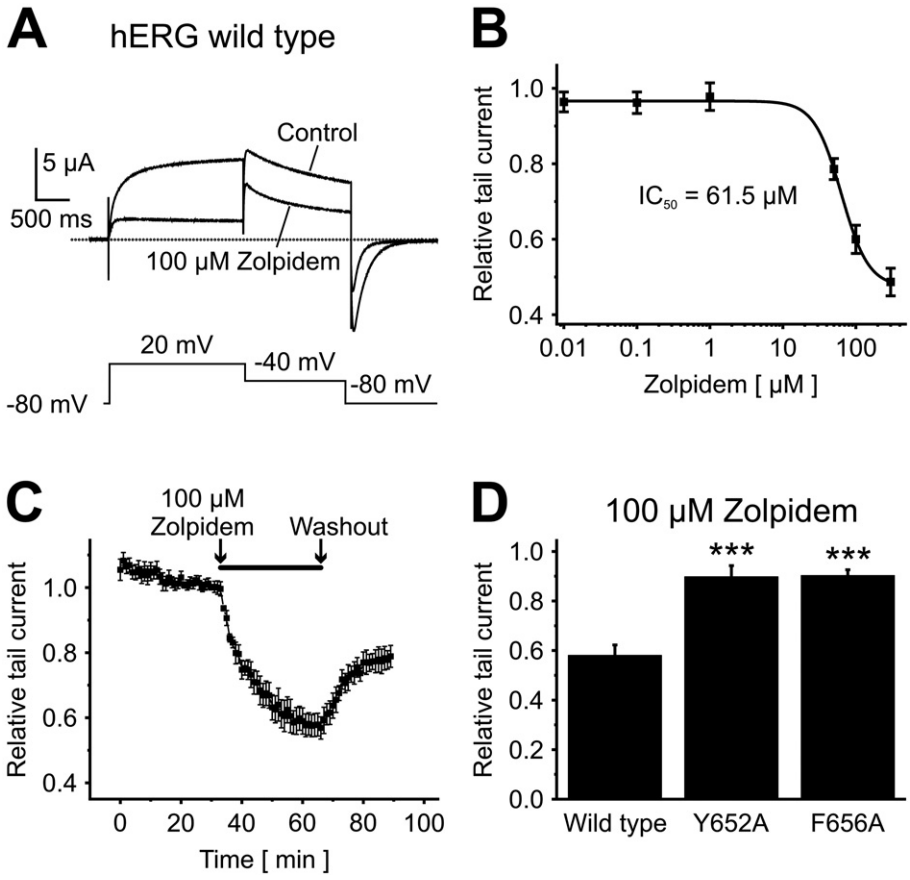

Figure 1

Acute hERG potassium channel blockade by zolpidem. (A) Representative current traces of hERG WT under control conditions and upon superfusion with 100 µM zolpidem for 30 min. (B) Concentration–response relationships for blockade of hERG tail currents (IC_{50} = 61.5 µM; n = 4–5). (C) The time course of block shows steady-state inhibition after 30 min and partial recovery from block during washout (n = 5). (D) Attenuation of block is achieved by mutating amino acids Y652 and F656 to alanine residues (n = 5 oocytes each). Data are given as mean ± SEM; ***P < 0.001. Dotted lines indicate zero current level.

parisons were performed using one-way ANOVA. If the hypothesis of equal means could be rejected at the 0.05 level, pairwise comparisons of groups were made, and the probability values were adjusted for multiple comparisons using the Bonferroni correction. Comparisons between action potential durations were performed using randomized block ANOVA followed by one-tailed Dunnett's test (α = 0.05).

Results

Acute inhibition of cardiac hERG K^+ channels by zolpidem

Zolpidem directly blocked hERG channels in *Xenopus* oocytes in a concentration-dependent manner (Figure 1A, B). Currents were activated by a 2 s depolarizing step to 20 mV followed by a repolarizing step to –40 mV for 1.6 s to produce outward tail currents that are characteristic of hERG potassium channels. The holding potential was –80 mV in all experiments, unless stated otherwise. Voltage pulses were applied at 10 s intervals during application of the drug solution for 30 min before the degree of block was determined (Figure 1A–C). To study the concentration dependence of hERG blockade by zolpidem, peak tail currents were measured in the presence of varying concentrations of the drug and normalized to their respective control values. Resulting means of relative current amplitudes are depicted in Figure 1B (n = 4–5 oocytes were investigated at each concentration). The half-maximal inhibitory concentration (IC_{50}) for block of tail currents yielded 61.5 ± 1.5 µM with a Hill coefficient (n_H) of 2.5 ± 0.18. The time course of block is shown in Figure 1C (n = 5). After a control period of 30 min illustrating stable current conditions, hERG channel block induced by 100 µM zolpidem reached a steady state after 30 min. The effect of 100 µM zolpidem on hERG was partially reversible upon washout (20 min).

Attenuation of zolpidem block by Y652A and F656A mutations

Aromatic residues Y652 and F656, located in the S6 domain of hERG, are critical determinants of drug binding to hERG channels (Mitcheson *et al.*, 2000; Thomas *et al.*, 2004b; El Harchi *et al.*, 2012). We investigated the effects of zolpidem

on mutant hERG Y652A and hERG F656A channels to assess the significance of these amino acid residues in channel blockade (Figure 1D). Currents were evoked as described (Figure 1A). Compared with 41.9 ± 4.2% reduction of hERG WT tail currents by 100 μM zolpidem (30 min), current inhibition was significantly attenuated in mutant hERG channels lacking the aromatic residues Y652 or F656 respectively (Y652A, 10.2 ± 4.5%, $n = 5$, $P = 0.0002$; F656A, 9.7 ± 2.3%, $n = 5$, $P = 0.0002$).

Zolpidem does not affect hERG channel activation

The effects of zolpidem on hERG activation current–voltage (*I–V*) relationship were investigated under isochronal recording conditions. Pulses were applied for 2.2 s to voltages between –80 and 80 mV in 10 mV increments (0.2 Hz) to activate hERG channels, and tail currents were recorded during a repolarizing voltage step to –40 mV for 1.6 s. Families of current traces are shown for control conditions and after exposure to 100 μM zolpidem for 30 min in Figure 2A, B. Currents measured at the end of the respective test pulse, activated at potentials greater than –50 mV, reached maximum values at 10 mV and then decreased at more positive potentials as a result of inactivation (Figure 2C, D). Figure 2E, F display activation curves (i.e. peak tail current amplitudes as a function of the preceding test pulse potential). hERG currents at the end of the test pulse to 10 mV were reduced by 54.5% ± 4.4% ($n = 4$; $P = 0.015$), and tail currents recorded at 80 mV were blocked by 46.8 ± 2.0% ($n = 4$; $P = 0.009$). The half-maximal activation voltage ($V_{1/2}$) was not significantly affected by zolpidem ($V_{1/2,control} = -8.2 \pm 0.77$ mV; $V_{1/2,zolpidem} = -8.5 \pm 1.9$ mV; $n = 4$; $P = 0.82$).

Effects of zolpidem on hERG inactivation

Zolpidem effects on inactivation of hERG channels were investigated using a dual approach. First, the influence of zolpidem on the time constant of inactivation was tested. Inactivating pulses to 40 mV were applied for 900 ms, followed by a brief repolarization to –100 mV for 16 ms causing rapid recovery from inactivation without inducing significant deactivation. During a second depolarizing pulse for 150 ms to voltages ranging from –40 to 40 mV (increment 20 mV), large, rapidly inactivating currents were evoked. Inactivating currents were recorded prior to (Figure 3A) and after blockade by 100 μM zolpidem (30 min; Figure 3B). The inactivation time constant depends on the current amplitude. Thus, one set of control cells and one set of matched oocytes after zolpidem application with similar mean current amplitudes at the end of the conditioning prepulse were compared ($I_{control}$ = 0.40 ± 0.03 μA vs. $I_{zolpidem}$ = 0.44 ± 0.07 μA; $n = 5$; $P = 0.61$). Single exponential fits to inactivating currents illustrate an apparent acceleration of hERG channel inactivation in the presence of zolpidem that reached statistical significance ($P = 0.03$; $n = 5$) at –20 mV membrane potential (Figure 3C).

To measure steady-state inactivation *I–V* relationships, channels were first inactivated at a holding potential of 20 mV followed by recovery from inactivation for 20 ms at potentials ranging from –110 to 30 mV (increment 10 mV) and by a second step to 20 mV. The latter voltage pulse evoked rapidly decaying outward tail currents, which were analysed as a measure of steady-state inactivation. After recording control measurements (Figure 3D), 100 μM zolpidem was applied for a period of 30 min, during which the holding potential was –80 mV in order to avoid destruction of the oocyte that occurs when permanently holding the cell at 20 mV. A typical recording in the presence of the drug is displayed in Figure 3E. The inactivating outward current amplitudes measured at 20 mV were normalized and plotted versus test pulse potentials, giving steady-state inactivation curves (Figure 3F). Mean half-maximal inactivation voltages ($V_{1/2}$) were not influenced by zolpidem ($V_{1/2,control} = -48.0 \pm 3.8$ mV; $V_{1/2,zolpidem} = -51.6 \pm 8.2$ mV; $n = 5$; $P = 0.52$).

State dependence of acute hERG current inhibition by zolpidem

State dependence of acute hERG current blockade (i.e. blockade in the closed, open and/or inactivated state) was assessed using two different protocols. The first protocol consisted of a long activating pulse, whereas the second protocol inactivated hERG channels prior to activation. In both protocols, we applied 100 μM zolpidem for 30 min while holding the cell in the closed state at –80 mV. Control measurements were performed prior to drug treatment (Figure 4A–D). First, we activated currents using a protocol with a single depolarizing step to 0 mV for 7.5 s to investigate whether the channel is blocked in the closed or activated (i.e. open and/or inactivated) state (Figure 4A). The degree of inhibition ($[1 - I_{zolpidem}/I_{control}] \times 100$) is displayed in Figure 4B. Analysis of the test pulse after drug application revealed a time-dependent increase of block to ~51% at 1000 ms in this representative cell, which is consistent with inhibition of activated hERG potassium channels. Please note that some degree of closed state block cannot be definitively ruled out by this protocol. In this series of experiments, hERG outward currents at the end of the 0 mV pulse were blocked by 53.7 ± 3.8% (100 μM zolpidem; $n = 5$).

Block of inactivated hERG channels was then addressed by application of a long inactivating test pulse to +80 mV (4 s) followed by a second voltage step (0 mV; 3.5 s) to open hERG channels. Typical current traces under control conditions and after application of 100 μM zolpidem are shown in Figure 4C. Figure 4D depicts normalized relative block upon channel opening during the second voltage pulse (0 mV), revealing that inhibition of hERG channels had already been obtained during the preceding inactivating +80 mV pulse. In contrast, weak additional time-dependent block of open channels was observed during the 0 mV pulse. Currents at the end of the second voltage step (0 mV) were reduced by 51.8 ± 3.7% ($n = 5$). These results are consistent with block of inactivated channels. In addition, a small fraction of channels that are in the open state at 80 mV may have been blocked as well. We conclude from these experiments that zolpidem binds to hERG channels in open and inactivated states.

Voltage dependence of block

To assess voltage dependence of zolpidem block, currents were elicited by a 34 s depolarizing pulse ranging from –40 to 80 mV followed by a second step to –100 mV for 2 s, during

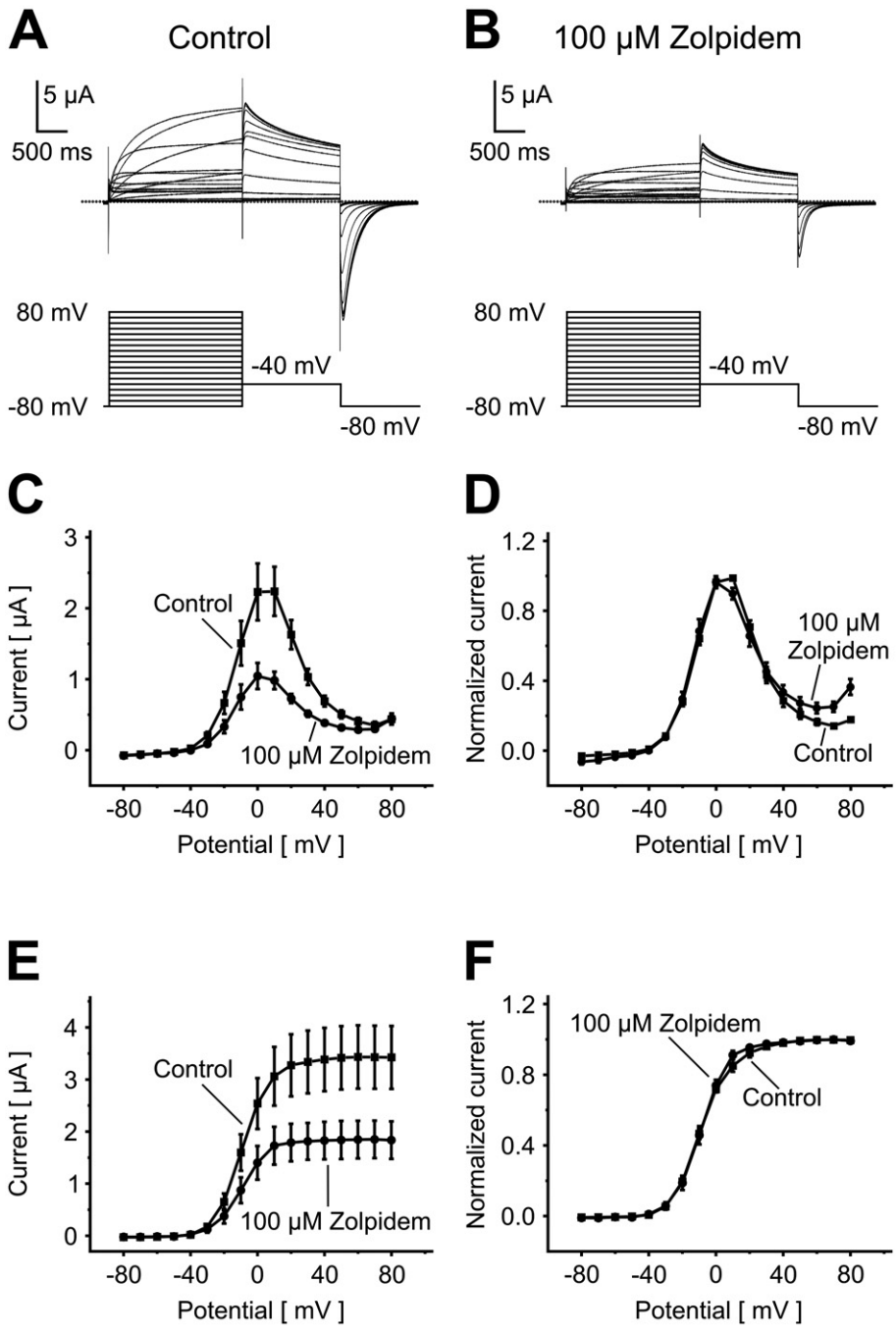

Figure 2

Voltage dependence of hERG activation. (A, B) Representative current traces under control conditions and after superfusion with 100 µM zolpidem are shown. (C, D) Mean current amplitudes at the end of the test pulse as function of the test pulse potential under control conditions and after incubation with zolpidem (C, original current amplitudes; D, values normalized to maximum step currents) ($n = 4$). (E, F) Activation curves (i.e. peak tail current amplitudes) as function of the preceding test pulse potential during the first step of the voltage protocol (E, original current amplitudes; F, values normalized to peak tail currents) ($n = 4$). The mean half-maximal activation potential $V_{1/2}$ was not significantly affected by zolpidem. Data are provided as mean ± SEM. Dotted lines indicate zero current level.

which peak inward tail currents were recorded. One specific test potential was studied per individual oocyte ($n = 5$ for each potential). Control currents were recorded before the cell was superfused with 100 µM zolpidem while holding hERG channels in the closed state at –80 mV for 30 min. Then measurements at the test pulse potential were performed, and relative inhibition of peak tail currents was plotted as a function of the preceding test pulse potential (Figure 4E). No significant

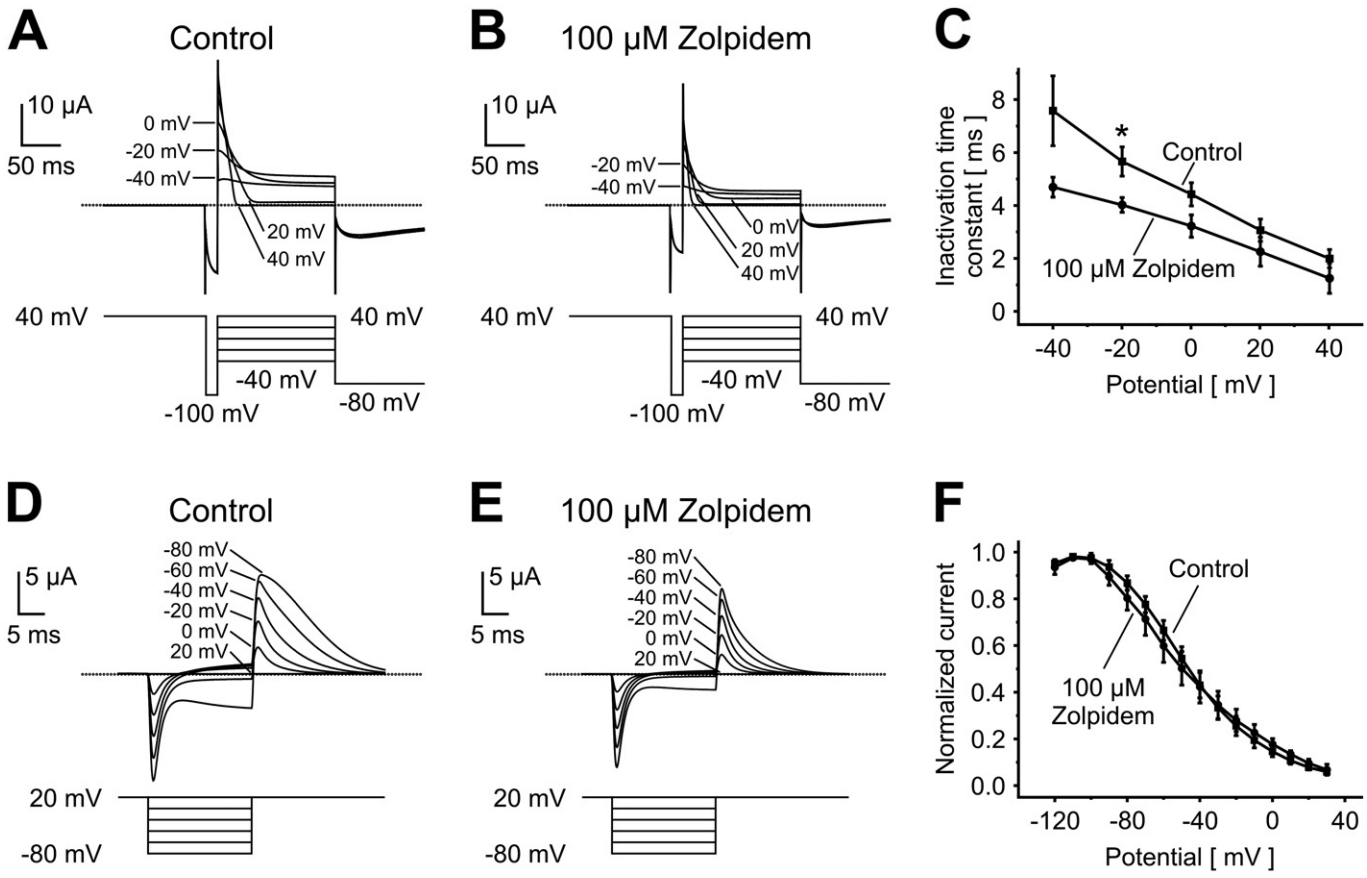

Figure 3

Zolpidem accelerates hERG channel inactivation. (A–C) Inactivation time constants were derived from exponentially decaying inactivating currents. Current measurements recorded from representative oocytes under control conditions (A) and after incubation with 100 µM zolpidem (B) are shown. (C) Mean inactivation time constants obtained from single-exponential fits to inactivating current traces ($n = 5$). (D, E) Inactivating currents were elicited by the constant step to 20 mV following potentials from −110 to 30 mV (increment, 10 mV). For clarity, not all original current traces are displayed. (F) Steady-state inactivation curves (i.e. normalized mean inactivating current amplitudes at 20 mV). The mean half-maximal inactivation voltage was not significantly shifted ($n = 5$). Data are given as mean ± SEM; *$P < 0.05$. Dotted lines indicate zero current level.

changes in tail current reduction were observed between the test pulse potentials applied.

hERG channel blockade by zolpidem is not frequency-dependent

Frequency dependence of block was investigated by rapidly activating hERG channels during a depolarizing voltage step to 20 mV for 300 ms, followed by a repolarizing step to −40 mV (300 ms) to elicit outward tail currents. Pulses were applied at frequencies of 1 and 0.1 Hz, respectively, during superfusion with 100 µM zolpidem (30 min). Each oocyte was studied at one stimulation rate only. The development of current reduction was plotted versus time (Figure 4F), and the resulting level of steady-state block served as a measure of the frequency dependence of block. The degree of steady-state inhibition at 1 Hz (41.1 ± 3.7%; $n = 5$) was not significantly different from 0.1 Hz (42.5 ± 2.8%; $n = 5$; $P = 0.77$), illustrating a frequency-independent mechanism of zolpidem-induced hERG channel blockade.

Acute and chronic effects of zolpidem on hERG channels expressed in a human cell line

While the *Xenopus* oocyte expression system is appropriate for mechanistic biophysical studies of hERG current inhibition, concentration–response relationships obtained from mammalian expression systems are required to evaluate the clinical relevance of drug effects (Redfern *et al.*, 2003). Thus, acute zolpidem block was studied in HEK 293 cells stably expressing hERG potassium channels. Channels were activated by a 2 s depolarization to +20 mV, and outward tail currents were recorded during a step to −50 mV for 2 s (Figure 5A). During wash-in of the drug, we applied this protocol at 0.1 Hz frequency until steady-state block was maintained for at least 30 s. hERG currents were blocked by zolpidem in a concentration-dependent manner (Figure 5B). The IC_{50} value for block of hERG tail currents was 65.5 ± 4.5 µM with a Hill coefficient n_H of 1.2 ± 0.14 (Figure 5B; n = 3–6 cells were studied at each concentration).

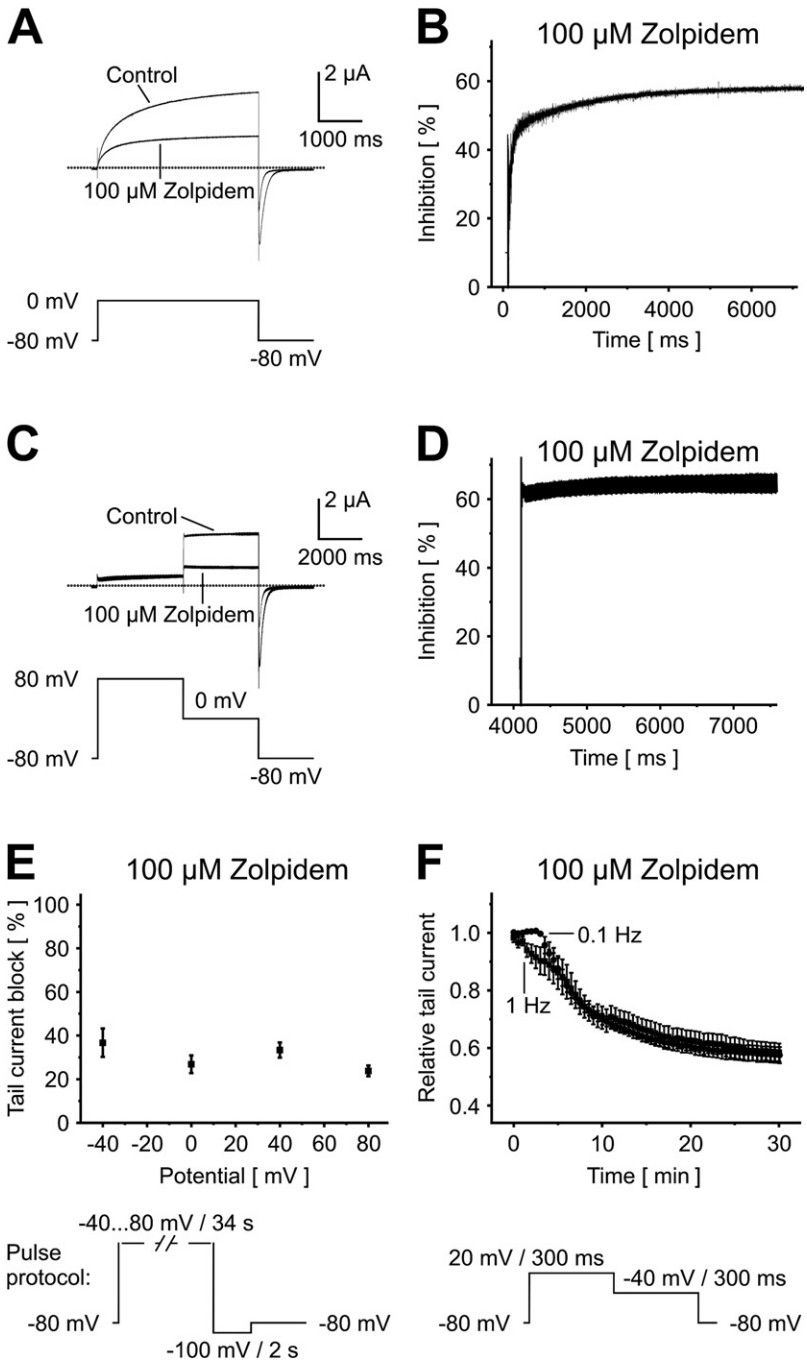

Figure 4

The biophysical mechanism of hERG current inhibition by zolpidem. (A–D) Block of activated hERG channels by zolpidem. (A, B) After recording the control measurement, the oocyte was clamped at –80 mV for 30 min during superfusion with the drug solution (100 µM zolpidem). The control recording and the first pulse measured after the incubation period are displayed (A). Panel B shows the degree of inhibition in %. Current inhibition increased time-dependently, illustrating that channel block occurs during opening and not in the preceding closed state. Similar results were observed in $n = 5$ experiments. (C, D) Inhibition of inactivated channels by 100 µM zolpidem. hERG channels were inactivated by a first voltage step to +80 mV, followed by channel opening at 0 mV. The corresponding relative block during the 0 mV step is displayed in panel D. Instantaneous inhibition (~60%) was observed, illustrating that channel block occurred during inactivation and increased only slightly when channels were subsequently opened. Representative current recordings of $n = 5$ experiments are depicted. (E) Zolpidem block of hERG is voltage-independent. The fraction of blocked peak tail currents is plotted as function of various test pulse potentials. Mean ± SEM hERG channel block did not differ between membrane voltages of –40, 0, 40 or 80 mV respectively ($n = 5$ cells each). (F) Lack of frequency dependence. Tail currents were analysed during the –40 mV step of the depicted voltage protocol. Resulting mean ± SEM relative tail current amplitudes (1 and 0.1 Hz stimulation rate; $n = 5$ oocytes were studied at each rate) during superfusion with 100 µM zolpidem for 30 min are plotted versus time. For the purpose of clear presentation, not all measurements are displayed. Dotted lines indicate zero current level.

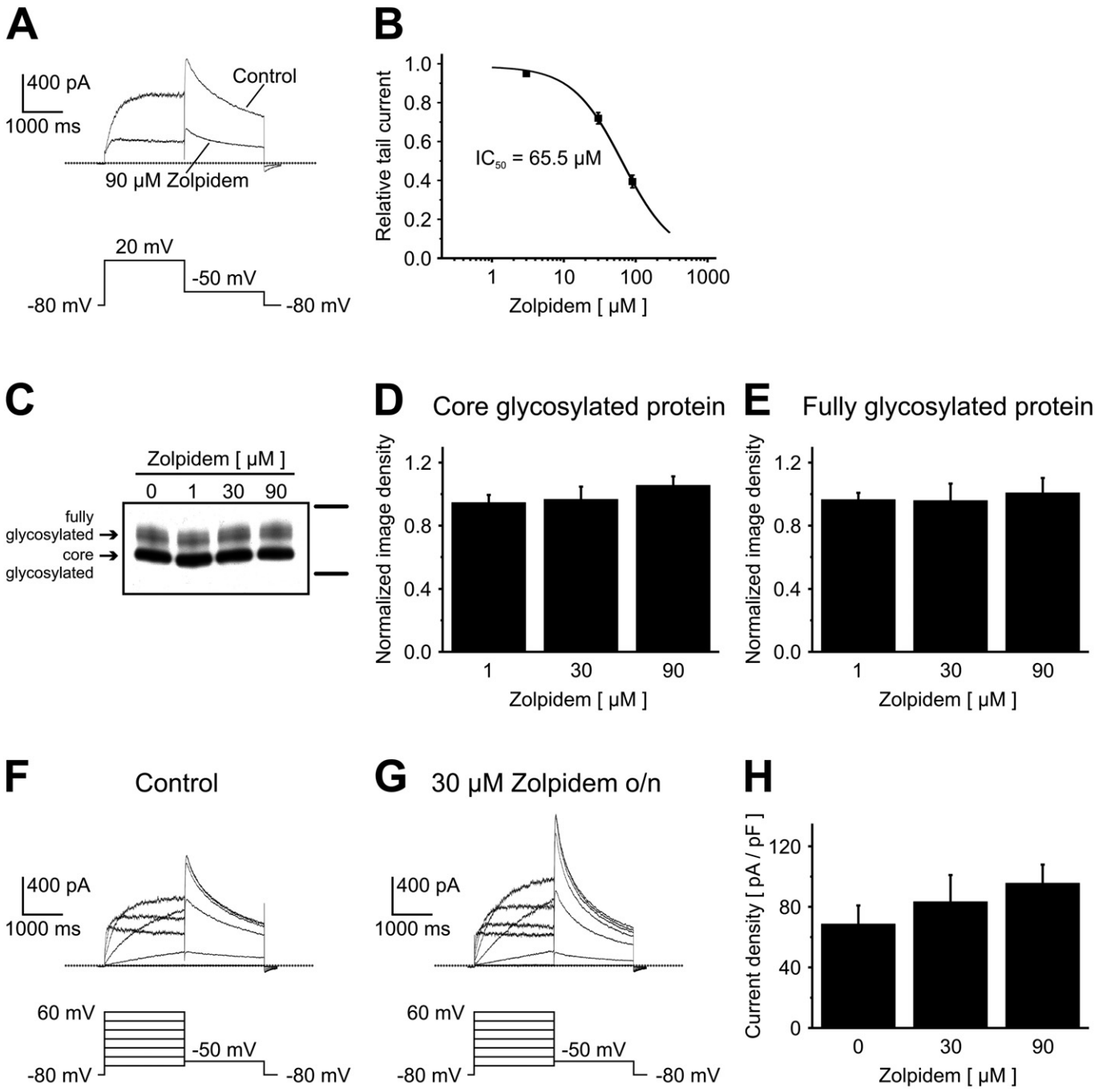

Figure 5

hERG currents and protein expression assessed in human cells. (A, B) Zolpidem blockade of hERG channels in HEK 293 cells. (A) Typical whole cell patch clamp recordings under control conditions and after application of 90 μM zolpidem. (B) Concentration–response curve for inhibition of hERG peak tail currents in HEK 293 cells, giving an IC_{50} value of 65.5 μM ($n = 3$–6 cells; error bars denote SEM). (C–E) Chronic zolpidem treatment did not affect maturation and surface expression of hERG protein. (C) Western blot analysis of hERG channel protein stably expressed in HEK 293 cells, with overnight exposure to increasing concentrations of zolpidem. (D, E) Western blot image density of immature core-glycosylated (D) and mature fully glycosylated hERG proteins (E), normalized to respective protein expression under drug-free conditions. Data were obtained from $n = 3$ experiments; upper marker, 200 kDa; lower marker, 122 kDa. (F–H) Prolonged exposure to zolpidem did not significantly affect I_{hERG} expressed in HEK 293 cells. Representative current recordings obtained under control conditions (F) and from cells treated overnight with 30 μM zolpidem (G) are shown. (H) Mean peak tail current densities. Data are given as mean ± SEM. Dotted lines indicate zero current level.

In addition to acute inhibition of functional hERG channels located in the plasma membrane, some hERG ligands have been revealed to decrease hERG currents chronically through impairment of protein trafficking to the cell surface (Ficker *et al.*, 2004; Rajamani *et al.*, 2006; Guo *et al.*, 2007; Takemasa *et al.*, 2007; Wang *et al.*, 2007; Staudacher *et al.*, 2010). hERG channels are synthesized in two forms, an immature core glycosylated protein of ~135 kDa that is localized in the endoplasmic reticulum (ER) and a fully glycosylated mature form of ~155 kDa, which is transported to the cell surface (Ficker *et al.*, 2003; Thomas *et al.*, 2003). To analyse zolpidem-induced changes in cell surface expression, we exposed HEK-hERG cells overnight (16–20 h) to increasing drug concentrations (1, 30, 90 μM) and tested for effects on hERG protein processing using Western blot analysis (Figure 5C). Compared to drug-free conditions, neither the expression of immature hERG protein (135 kDa band; Figure 5D) nor the levels of mature hERG protein (155 kDa band; Figure 5E) were significantly affected by zolpidem treatment in n = 3 assays. Consistent with preserved hERG cell surface expression, macroscopic current amplitudes were not reduced by chronic zolpidem treatment (Figure 5F–H). Pulses were applied for 2 s to voltages between –60 and +60 mV in 20 mV increments (0.1 Hz), and tail currents were analysed during a constant repolarizing step to –50 mV for 2 s. Families of hERG current traces from one cell are shown for control conditions and after overnight exposure to 30 μM zolpidem (Figure 5F, G). Following incubation with zolpidem, the drug was washed out for 1 h prior to electrophysiological recordings to allow for recovery from acute block. Mean current densities were not significantly different after overnight zolpidem treatment (30 μM, 83.4 ± 17.6 pA/pF, n = 8, P = 0.49; 90 μM, 95.6 ± 12.2 pA/pF, n = 8, P = 0.14) compared with control conditions (68.7 ± 12.3 pA/pF; n = 10) (Figure 5H).

Zolpidem causes action potential prolongation in human cardiomyocytes derived from induced pluripotent stem cells

To validate whether the observed *in vitro* actions of zolpidem are relevant to cardiac electrophysiology, effects of the drug on action potentials were studied in hiPSC-derived cardiac myocytes (Ma *et al.*, 2011). Zolpidem (10 and 30 μM) was applied acutely until steady-state conditions were achieved, resulting in prolongation of APD_{90} from 321.2 ± 45.5 ms (n = 9) in the absence of the drug to 375.8 ± 55.5 ms (10 μM; n = 9; $P < 0.05$) and to 414.1 ± 54.8 ms (30 μM; n = 9; $P < 0.05$) after zolpidem exposure respectively (Figure 6A, B). APD_{50} was not significantly affected (Figure 6A, C). These results indicate that acute zolpidem administration induces cardiac action potential changes that are consistent with clinically observed QT prolongation.

TdP have been observed during the clinical use of zolpidem in combination with the class III anti-arrhythmic drug amiodarone (Letsas *et al.*, 2006). Amiodarone is a multichannel blocker that prolongs the cardiac action potential primarily through inhibition of hERG channels (Kiehn *et al.*, 1999; Zhang *et al.*, 2010). Thus, we next assessed a cumulative effect of zolpidem and amiodarone on action potential duration. When applied separately, amiodarone caused prolongation of APD_{90} from 287.5 ± 30.8 ms (n = 8) under baseline conditions to 328.4 ± 37.5 ms (10 nM; n = 8; $P > 0.05$), 349.6 ± 50.4 ms (100 nM; n = 8; $P < 0.05$) and 403.0 ± 59.1 ms (1 μM; n = 7; $P < 0.05$) respectively (Figure 6D, E). APD_{50} was not significantly affected by amiodarone (Figure 6D, F). Amiodarone (100 nM) and zolpidem were then co-administered to study potential additive effects of both drugs. Compared with APD_{90} during amiodarone treatment (341.0 ± 45.3 ms; n = 8), zolpidem caused additional action potential prolongation to 381.3 ± 38.1 ms (10 μM; n = 8; $P > 0.05$) and to 450.3 ± 50.2 ms (30 μM; n = 8; $P < 0.05$) in this series of experiments (Figure 6G, H).

Zolpidem is not associated with apoptotic cell death

Recently, a novel mechanism leading to hERG-associated cardiac adverse effects was revealed. Pharmacological inhibition of hERG channels has been shown to promote apoptosis (Thomas *et al.*, 2008; Obers *et al.*, 2010; Jehle *et al.*, 2011; Staudacher *et al.*, 2011a). To assess whether zolpidem exerts similar actions, apoptotic cell death was studied in HL-1 cells using TUNEL staining (Figure 7). Cells were cultured in drug-free control media or in the presence of 100 and 300 μM zolpidem for 24 h. Compared with medium-treated controls, similarly low degrees of apoptosis were detected following administration of zolpidem (Figure 7A–F; n = 4 assays).

Discussion

Zolpidem has been associated with acquired LQTS that is most commonly related to hERG K^+ channel dysfunction. Effects of zolpidem on hERG channels have not been reported prior to this study. The present in-depth assessment of hERG-related cardiac adverse effects reveals that zolpidem causes APD prolongation in hiPSC-derived cardiomyocytes and inhibits hERG currents in *X. laevis* oocytes (IC_{50} = 61.5 μM) and HEK 293 cells (IC_{50} = 65.5 μM). In most cases, IC_{50} values for hERG channel block are 3- to 20-fold higher when the drug is applied to the extracellular surface of *Xenopus* oocytes compared with mammalian cells (Obers *et al.*, 2010). It is noteworthy that zolpidem differs from this observation, exhibiting similar IC_{50} values in both expression systems. One possible explanation is the use of relatively long incubation times in oocyte experiments of this study that could enable drug equilibration. In addition, this phenomenon may be attributed to specific physicochemical properties of zolpidem.

Biophysical mechanism of acute hERG current blockade by zolpidem

Biophysical characteristics of hERG current inhibition were elucidated in detail. Zolpidem blocked hERG channels in the open and inactivated states, as demonstrated using voltage protocols designed to discriminate between open, closed and inactivated states (Figure 4A–D). It is important to take into consideration that there is no approach allowing for specific analysis of open, closed or inactivated channels in isolation. As a result, each assessment of state-dependent hERG channel blockade will be an approximation. In particular, limitations arise from potential inhibition of closed channels, since at

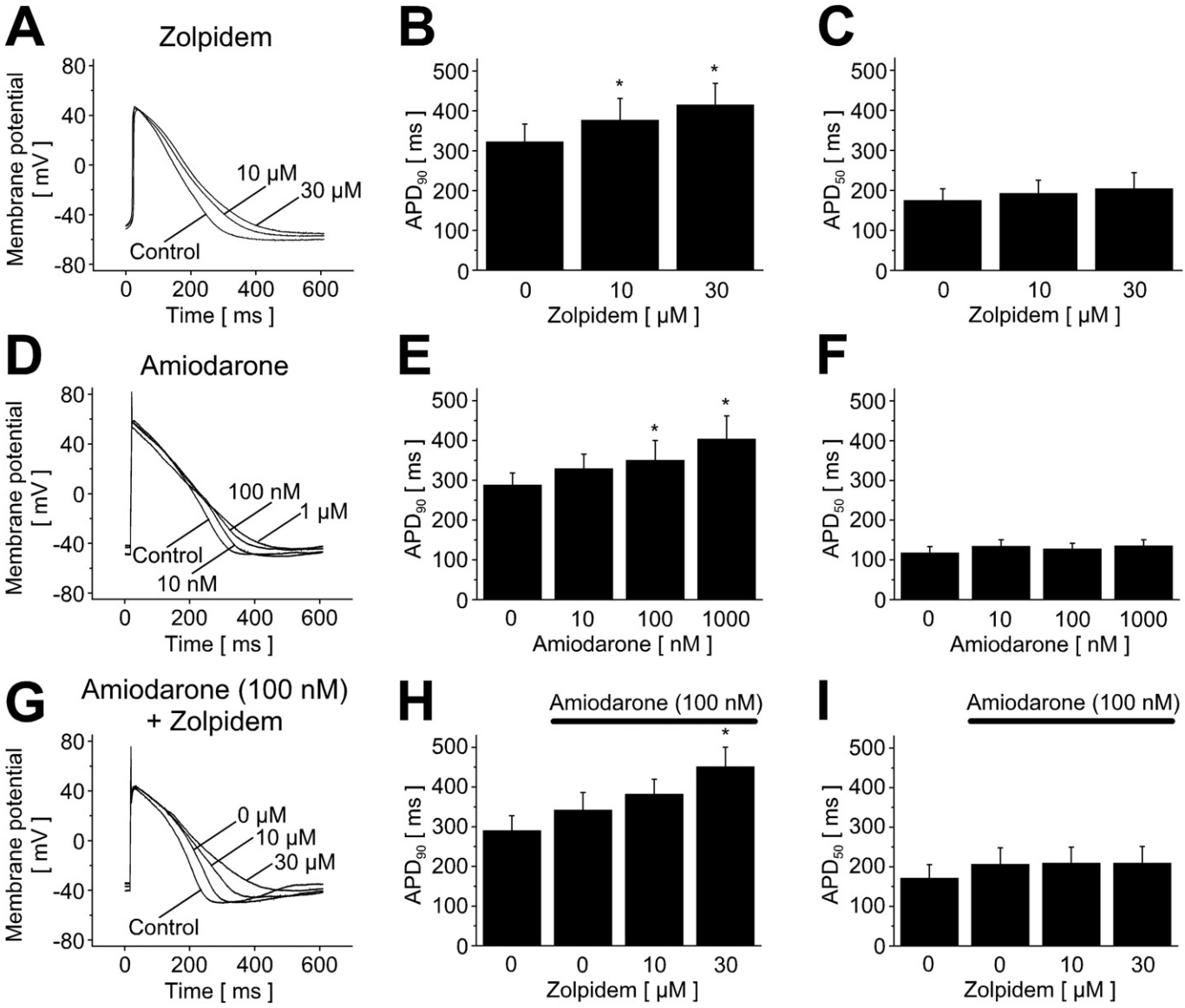

Figure 6

Acute effects of zolpidem and amiodarone on action potential duration in human cardiac myocytes derived from induced pluripotent stem cells. (A) Representative current clamp recordings of actions potentials under control conditions and after extracellular perfusion with zolpidem (10 and 30 µM) are displayed. (B, C) Quantitative analysis of mean ± SEM action potential duration (B, APD_{90}; C, APD_{50}) recorded from cardiomyocytes upon acute exposure to zolpidem. (D–F) Action potential prolongation associated with amiodarone (D, original action potential recordings; E, F, mean APD_{90} or APD_{50} values). (G–I) Additive effects of zolpidem and amiodarone on the cardiac action potential duration. Panel G depicts representative recordings, illustrating additional APD_{90} prolongation caused by 30 µM zolpidem (H) in the presence of 100 nM amiodarone. APD_{50} was not affected (I). *$P < 0.05$ versus control conditions (B, E) or 100 nM amiodarone (H) respectively.

0 mV or at 80 mV a small fraction of channels are statistically expected to occupy the closed state, and zolpidem binding to closed channels may therefore contribute to macroscopic current inhibition. Zolpidem application accelerated hERG current inactivation, which is expected to contribute to macroscopic current reduction (Figure 3A–C). In contrast, current–voltage relationships of channel activation or inactivation were not affected (Figure 2 and 3). Unblocking upon repolarization, which allows hERG channels to become available for opening, occurred rather slowly, and a complete washout could not be achieved in oocytes (Figure 1). However, the lack of frequency dependence (Figure 4F) argues against significant accumulation of block in between voltage pulses.

Structural determinants of the hERG drug binding site have been revealed in the past. Aromatic rings of amino acid residues Y652 and F656 located in the S6 domain support drug binding (Mitcheson *et al.*, 2000), and mutation of these residues dramatically reduces the potency of several drugs tested to date (for review, see Thomas *et al.*, 2006; Staudacher *et al.*, 2010). Reduced hERG Y652A and hERG F656A current inhibition by zolpidem (Figure 1D) shows that the drug binds

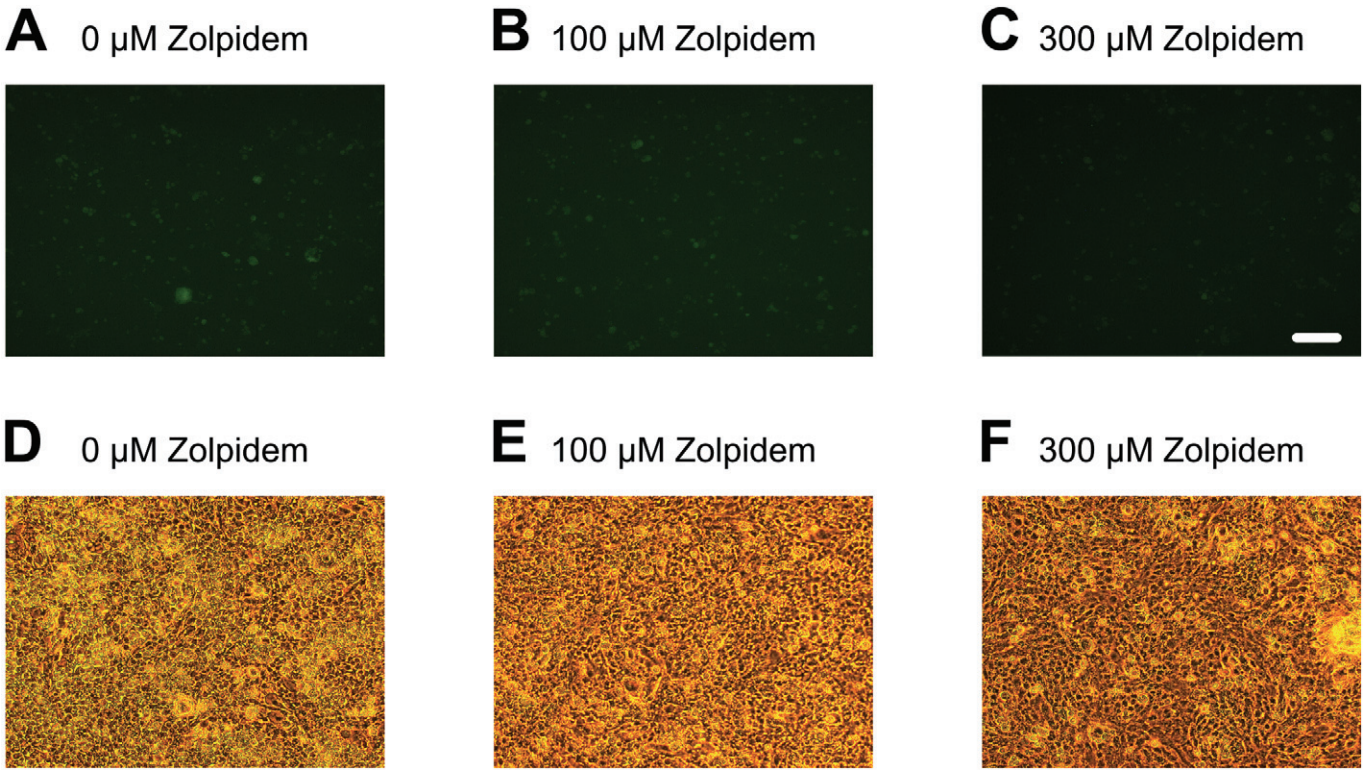

Figure 7

Zolpidem does not induce apoptosis in HL-1 cardiac myocytes. HL-1 cells were exposed to zolpidem (B, E, 100 μM; C, F, 300 μM) for 24 h. (A–C) Fluorescence microphotographs corresponding to TUNEL assays. Apoptotic cells show increased green nuclear fluorescence reflecting endonucleolytic DNA degradation. No apparent increase in green fluorescence was detected after treatment with 100 μM (B) or 300 μM zolpidem (C) relative to medium-treated control cells (A). Conventional microphotographs illustrate 100% HL-1 cell confluency under control conditions (D) and upon exposure to 100 μM zolpidem (E) and 300 μM zolpidem (F) for 24 h (cells were ~80% confluent at the beginning of drug treatment). Scale bar, 100 μm.

to this drug receptor within the pore-S6 region. Furthermore, the lack of voltage dependence (Figure 4E) indicates that drug access to the binding site does not rely on a specific conformation of the channel pore.

Zolpidem does not affect hERG protein expression

In addition to acute current blockade, inhibitors of hERG channels may reduce I_{Kr} by selective disruption of hERG protein trafficking into the cell surface membrane, a mechanism that has been reported for several compounds (Staudacher *et al.*, 2010). Chronic zolpidem application did not affect hERG channel surface expression (Figure 5C–E), indicating that pharmacological current inhibition is the sole mechanism of zolpidem-induced hERG current reduction. This finding suggests different drug–channel interaction sites for inhibition of hERG forward trafficking and acute blockade respectively.

Lack of pro-apoptotic effects despite inhibition of hERG potassium channels

Pro-apoptotic effects have been observed with low-affinity hERG current inhibitors (Thomas *et al.*, 2008; Gong *et al.*, 2010; Obers *et al.*, 2010; Staudacher *et al.*, 2011a). In contrast, zolpidem did not affect apoptosis of HL-1 cardiac myocytes. Different effects of hERG inbibitors on cell apoptosis suggest compound- and/or cell-specific molecular mechanisms of hERG-associated apoptosis that remain to be elucidated in detail (Jehle *et al.*, 2011).

Physiological significance and clinical implications

Action potential recordings provide an integrated approach to evaluate the complex action of zolpidem on multiple cellular factors that contribute to cardiac repolarization. Specifically, cardiomyocytes derived from hiPSC have been used successfully to study mechanisms of long QT syndrome (Caspi *et al.*, 2009; Moretti *et al.*, 2010; Peng *et al.*, 2010; Itzhaki *et al.*, 2011). Here, zolpidem caused prolongation of action potentials recorded from hiPSC-derived cardiomyocytes (Figure 6) in mechanistic accordance with clinical QT interval prolongation (Letsas *et al.*, 2006). Zolpidem prolonged APD_{90} without significantly affecting APD_{50}, resulting in triangulation of the shape of the action potential (Figure 6), which has been previously identified as pro-arrhythmic predictor (Hondeghem, 2008).

Based on the analysis of *in vitro* data and clinical drug effects, a 30-fold safety margin between free drug concentra-

tion and the experimental IC_{50} value obtained from mammalian cells was suggested as indicator of pro-arrhythmic safety of a drug. Zolpidem plasma concentrations range from 0.19 to 0.50 μM (Drover, 2004; Greenblatt *et al.*, 2006; De Haas *et al.*, 2010). Since zolpidem is approximately 92% plasma bound (Salvà and Costa, 1995), effective free drug concentrations are by ~10-fold lower. Considering the hERG IC_{50} value of 65.5 μM and APD prolongation observed at 10 μM, the calculated zolpidem safety factor ranges from 1310 to 3447 (200–526 for APD prolongation), suggesting an extremely low pro-arrhythmic potential during routine therapeutic drug use that corresponds well with the rare clinical incidence of zolpidem-induced LQTS. However, cardiac safety of psychotropic compounds should extend to cases of drug overdose. Excessive daily zolpidem doses of up to 1200 mg and blood concentrations of 11.3 μM (free concentration, ~1.13 μM) have been reported (Hajak *et al.*, 2003; Jones *et al.*, 2007). The resulting safety factors of 58 for hERG inhibition and 9 for APD prolongation indicate clinical significance in these cases. Similarly, the presence of additional conditions that reduce the repolarization reserve (Roden, 2008) is expected to precipitate LQTS during zolpidem treatment. Indeed, the case reported by Letsas *et al.* (2006) links LQTS and TdP to the simultaneous administration of zolpidem and the hERG inhibitor amiodarone (Kiehn *et al.*, 1999). We found additive effects of zolpidem and amiodarone on APD in hiPSC-derived cardiomyocytes (Figure 6), providing a mechanistic basis for this clinical observation. In addition, metabolic interactions may elevate zolpidem plasma concentrations towards critical levels. Because zolpidem is metabolized by CYP3A4, CYP3A4 loss of function mutations may account for increased zolpidem levels despite drug application according to prescription. Furthermore, competition of CYP3A4 substrates for binding to its catalytic subunit may result in impaired metabolism of affected compounds, leading to plasma level elevation. Specifically, co-application of zolpidem and amiodarone may interfere with the hepatic metabolism of both compounds, resulting in enhanced QT prolonging effects of the drugs.

Conclusion

Zolpidem inhibits cardiac hERG K^+ channels and causes APD prolongation. Despite a relatively low hERG channel affinity, APD prolongation may lead to acquired LQTS and TdP in cases of reduced repolarization reserve or zolpidem overdose. In contrast to other compounds that cause acute hERG current blockade, zolpidem lacks hERG-related long-term effects (i.e. induction of apoptosis and inhibition of protein trafficking), revealing a unique profile with respect to hERG pharmacology. Further studies are required to elucidate the complex relationship among electrophysiological, biochemical and cellular effects of hERG inhibition.

Acknowledgements

We thank William C Claycomb (New Orleans) for providing HL-1 cells; and we are grateful to Jennifer Gütermann, Christine Jeckel, Bianca Stadler and Kai Sona for excellent technical assistance. This work was supported by grants from the German Heart Foundation/German Foundation of Heart Research (Kaltenbach Scholarships to JJ and FW, project F/06/10 to DT), from the Joachim Siebeneicher Foundation (to DT), from the DZHK (Deutsches Zentrum für Herz-Kreislauf-Forschung – German Centre for Cardiovascular Research) and the BMBF (German Ministry of Education and Research) (to DT), from the National Institutes of Health (HL71789 to EF and HL94450 to ID), from the Amercian Heart Association (12EIA9300060 to ID) and from the Max-Planck-Society (TANDEM project to PAS).

Conflict of interest

None.

References

Alexander SP, Mathie A, Peters JA (2011). Guide to Receptors and Channels (GRAC), 5th edition. Br J Pharmacol 164 (Suppl. 1): S1–S324.

Bianchi L, Wible B, Arcangeli A, Tagliatatela M, Morra F, Castaldo P *et al.* (1998). Herg encodes a K^+ current highly conserved in tumors of different histogenesis: a selective advantage for cancer cells? Cancer Res 58: 815–822.

Caspi O, Itzhaki I, Kehat I, Gepstein A, Arbel G, Huber I *et al.* (2009). In vitro electrophysiological drug testing using human embryonic stem cell derived cardiomyocytes. Stem Cells Dev 18: 161–172.

Cherubini A, Taddei GL, Crociani O, Paglierani M, Buccoliero AM, Fontana L *et al.* (2000). HERG potassium channels are more frequently expressed in human endometrial cancer as compared to non-cancerous endometrium. Br J Cancer 83: 1722–1729.

Claycomb WC, Lanson NA Jr, Stallworth BS, Egeland DB, Delcarpio JB, Bahinski A *et al.* (1998). HL-1 cells: a cardiac muscle cell line that contracts and retains phenotypic characteristics of the adult cardiomyocyte. Proc Natl Acad Sci U S A 95: 2979–2984.

De Haas SL, Schoemaker RC, van Gerven JM, Hoever P, Cohen AF, Dingemanse J (2010). Pharmacokinetics, pharmacodynamics and the pharmacokinetic/ pharmacodynamic relationship of zolpidem in healthy subjects. J Psychopharmacol 24: 1619–1629.

Dennis AT, Nassal D, Deschenes I, Thomas D, Ficker E (2011). Antidepressant-induced ubiquitination and degradation of the cardiac potassium channel hERG. J Biol Chem 286: 34413–34425.

Drover DR (2004). Comparative pharmacokinetics and pharmacodynamics of short-acting hypnosedatives: zaleplon, zolpidem and zopiclone. Clin Pharmacokinet 43: 227–238.

Dündar Y, Boland A, Strobl J, Dodd S, Haycox A, Bagust A *et al.* (2004). Newer hypnotic drugs for the short-term management of insomnia: a systematic review and economic evaluation. Health Technol Assess 8: 1–125.

El Harchi A, Zhang YH, Hussein L, Dempsey CE, Hancox JC (2012). Molecular determinants of hERG potassium channel inhibition by disopyramide. J Mol Cell Cardiol 52: 185–195.

Ficker E, Dennis AT, Wang L, Brown AM (2003). Role of cytosolic chaperones Hsp70 and Hsp90 in maturation of the cardiac potassium channel HERG. Circ Res 92: e87–e100.

Ficker E, Kuryshev YA, Dennis AT, Obejero-Paz C, Wang L, Hawryluk P *et al.* (2004). Mechanisms of arsenic-induced prolongation of cardiac repolarization. Mol Pharmacol 66: 33–44.

Gierten J, Ficker E, Bloehs R, Schlömer K, Kathöfer S, Scholz E *et al.* (2008). Regulation of two-pore-domain (K_{2P}) potassium leak channels by the tyrosine kinase inhibitor genistein. Br J Pharmacol 154: 1680–1690.

Gong JH, Liu XJ, Shang BY, Chen SZ, Zhen YS (2010). HERG K+ channel related chemosensitivity to sparfloxacin in colon cancer cells. Oncol Rep 23: 1747–1756.

Greenblatt DJ, Legangneux E, Harmatz JS, Weinling E, Freeman J, Rice K *et al.* (2006). Dynamics and kinetics of a modified-release formulation of zolpidem: comparison with immediate-release standard zolpidem and placebo. J Clin Pharmacol 46: 1469–1480.

Guo J, Massaeli H, Li W, Xu J, Luo T, Shaw J *et al.* (2007). Identification of I_{Kr} and its trafficking disruption induced by probucol in cultured neonatal rat cardiomyocytes. J Pharmacol Exp Ther 321: 911–920.

Hajak G, Müller WE, Wittchen HU, Pittrow D, Kirch W (2003). Abuse and dependence potential for the non-benzodiazepine hypnotics zolpidem and zopiclone: a review of case reports and epidemiological data. Addiction 98: 1371–1378.

Hausken AM, Furu K, Skurtveit S, Engeland A, Bramness JG (2009). Starting insomnia treatment: the use of benzodiazepines versus z-hypnotics. A prescription database study of predictors. Eur J Clin Pharmacol 65: 295–301.

Hondeghem LM (2008). Use and abuse of QT and TRIaD in cardiac safety research: importance of study design and conduct. Eur J Pharmacol 584: 1–9.

Itzhaki I, Maizels L, Huber I, Zwi-Dantsis L, Caspi O, Winterstern A *et al.* (2011). Modelling the long QT syndrome with induced pluripotent stem cells. Nature 471: 225–229.

Jehle J, Schweizer PA, Katus HA, Thomas D (2011). Novel roles for hERG K(+) channels in cell proliferation and apoptosis. Cell Death Dis 2: e193.

Jones AW, Holmgren A, Kugelberg FC (2007). Concentrations of scheduled prescription drugs in blood of impaired drivers: considerations for interpreting the results. Ther Drug Monit 29: 248–260.

Kiehn J, Thomas D, Karle CA, Schöls W, Kübler W (1999). Inhibitory effects of the class III antiarrhythmic drug amiodarone on cloned HERG potassium channels. Naunyn Schmiedebergs Arch Pharmacol 359: 212–219.

Lacerda AE, Kramer J, Shen KZ, Thomas D, Brown AM (2001). Comparison of block among cloned cardiac potassium channels by non-antiarrhythmic drugs. Eur Heart J 3 (Suppl. K): K23–K30.

Letsas KP, Filippatos GS, Kounas SP, Efremidis M, Sideris A, Kardaras F (2006). QT interval prolongation and Torsades de Pointes in a patient receiving zolpidem and amiodarone. Cardiology 105: 146–147.

Lugenbiel P, Bauer A, Kelemen K, Schweizer PA, Becker R, Katus HA *et al.* (2012). Biological heart rate reduction through genetic suppression of $G\alpha_s$ protein in the sinoatrial node. J Am Heart Assoc 1: jah3-e000372.

Ma J, Guo L, Fiene SJ, Anson BD, Thomson JA, Kamp TJ *et al.* (2011). High purity human-induced pluripotent stem cell-derived cardiomyocytes: electrophysiological properties of action potentials and ionic currents. Am J Physiol Heart Circ Physiol 301: H2006–H2017.

McGrath J, Drummond G, Kilkenny C, Wainwright C (2010). Guidelines for reporting experiments involving animals: the ARRIVE guidelines. Br J Pharmacol 160: 1573–1576.

Mitcheson JS, Chen J, Lin M, Culberson C, Sanguinetti MC (2000). A structural basis for drug-induced long QT syndrome. Proc Natl Acad Sci U S A 97: 12329–12333.

Moretti A, Bellin M, Welling A, Jung CB, Lam JT, Bott-Flügel L *et al.* (2010). Patient-specific induced pluripotent stem-cell models for long-QT syndrome. N Engl J Med 363: 1397–1409.

Nicholson AN, Pascoe PA (1986). Hypnotic activity of an imidazo-pyridine (zolpidem). Br J Clin Pharmacol 21: 205–211.

Obers S, Staudacher I, Ficker E, Dennis A, Koschny E, Erdal H *et al.* (2010). Multiple mechanisms of hERG liability: K+ current inhibition, disruption of protein trafficking, and apoptosis induced by amoxapine. Naunyn Schmiedebergs Arch Pharmacol 381: 385–400.

Peng S, Lacerda AE, Kirsch GE, Brown AM, Bruening-Wright A (2010). The action potential and comparative pharmacology of stem cell-derived human cardiomyocytes. J Pharmacol Toxicol Methods 61: 277–286.

Rajamani S, Eckhardt LL, Valdivia CR, Klemens CA, Gillman BM, Anderson CL *et al.* (2006). Drug-induced long QT syndrome: hERG K+ channel block and disruption of protein trafficking by fluoxetine and norfluoxetine. Br J Pharmacol 149: 481–489.

Redfern WS, Carlsson L, Davis AS, Lynch WG, MacKenzie I, Palethorpe S *et al.* (2003). Relationships between preclinical cardiac electrophysiology, clinical QT interval prolongation and torsade de pointes for a broad range of drugs: evidence for a provisional safety margin in drug development. Cardiovasc Res 58: 32–45.

Roden D (2008). Repolarization reserve: a moving target. Circulation 118: 981–982.

Salvà P, Costa J (1995). Clinical pharmacokinetics and pharmacodynamics of zolpidem. Therapeutic implications. Clin Pharmacokinet 29: 142–153.

Sanguinetti MC, Tristani-Firouzi M (2006). hERG potassium channels and cardiac arrhythmia. Nature 440: 463–469.

Seyler C, Duthil-Straub E, Zitron E, Gierten J, Scholz EP, Fink RH *et al.* (2012). TASK1 (K_{2P}3.1) K+ current inhibition by endothelin-1 is mediated by Rho kinase-dependent channel phosphorylation. Br J Pharmacol 165: 1467–1475.

Smith GAM, Tsui HW, Newell EW, Jiang X, Zhu XP, Tsui FWL *et al.* (2002). Functional up-regulation of HERG K^+ channels in neoplastic hematopoietic cells. J Biol Chem 277: 18528–18534.

Soucek R, Thomas D, Kelemen K, Bikou O, Seyler C, Voss F *et al.* (2012). Genetic suppression of atrial fibrillation using a dominant-negative ether-a-go-go-related gene mutant. Heart Rhythm 9: 265–272.

Staudacher I, Schweizer PA, Katus HA, Thomas D (2010). hERG: protein trafficking and potential for drug side effects. Curr Opin Drug Discov Devel 13: 23–30.

Staudacher I, Wang L, Wan X, Obers S, Wenzel W, Tristram F *et al.* (2011a). hERG K+ channel-associated cardiac effects of the antidepressant drug desipramine. Naunyn Schmiedebergs Arch Pharmacol 383: 119–139.

Staudacher K, Staudacher I, Ficker E, Seyler C, Gierten J, Kisselbach J *et al.* (2011b). Carvedilol targets human K_{2P}3.1 (TASK1) K+ leak channels. Br J Pharmacol 163: 1099–1110.

Takemasa H, Nagatomo T, Abe H, Kawakami K, Igarashi T, Tsuguri T *et al.* (2007). Coexistence of hERG current block and

disruption of protein trafficking in ketoconazole-induced long QT syndrome. Br J Pharmacol 153: 439–447.

Thomas D, Zhang W, Karle CA, Kathöfer S, Schöls W, Kübler W *et al*. (1999). Deletion of protein kinase a phosphorylation sites in the HERG potassium channel inhibits activation shift by protein kinase A. J Biol Chem 274: 27457–27462.

Thomas D, Wendt-Nordahl G, Röckl K, Ficker E, Brown AM, Kiehn J (2001). High affinity blockade of HERG human cardiac potassion channels by the novel antiarrhythmic drug BRL-32872. J Pharmacol Exp Ther 297: 735–761.

Thomas D, Kiehn J, Katus HA, Karle CA (2003). Defective protein trafficking in hERG-associated hereditary long QT syndrome (LQT2): molecular mechanisms and restoration of intracellular protein processing. Cardiovasc Res 60: 235–241.

Thomas D, Gut B, Karsai S, Wimmer AB, Wu K, Wendt-Nordahl G *et al*. (2004a). Inhibition of cloned HERG potassium channels by the antiestrogen tamoxifen. Naunyn Schmiedebergs Arch Pharmacol 368: 41–48.

Thomas D, Wimmer AB, Wu K, Hammerling BC, Ficker EK, Kuryshev YA *et al*. (2004b). Inhibition of human ether-a-go-go-related gene potassium channels by alpha 1-adrenoceptor antagonists prazosin, doxazosin, and terazosin. Naunyn Schmiedebergs Arch Pharmacol 369: 462–472.

Thomas D, Karle CA, Kiehn J (2006). The cardiac hERG/I_{Kr} potassium channel as pharmacological target: structure, function, regulation, and clinical applications. Curr Pharm Des 12: 2271–2283.

Thomas D, Bloehs R, Koschny R, Ficker E, Sykora J, Kiehn J *et al*. (2008). Doxazosin induces apoptosis of cells expressing hERG potassium channels. Eur J Pharmacol 579: 98–103.

Trappe K, Thomas D, Bikou O, Kelemen K, Lugenbiel P, Voss F *et al*. (2012). Suppression of persistent atrial fibrillation by genetic knockdown of caspase 3 – a preclinical pilot study. Eur Heart J doi:10.1093/eurheartj/ehr269.

Van der Heyden MAG, Smits ME, Vos MA (2008). Drugs and trafficking of ion channels: a new pro-arrhythmic threat on the horizon? Br J Pharmacol 153: 406–409.

Viskin S (1999). Long QT syndromes and torsade de pointes. Lancet 354: 1625–1633.

Wang H, Zhang Y, Cao L, Han H, Wang J, Yang B *et al*. (2002). HERG K+ channel, a regulator of tumor cell apoptosis and proliferation. Cancer Res 62: 4843–4848.

Wang L, Wible BA, Wan X, Ficker E (2007). Cardiac glycosides as novel inhibitors of human ether-a-go-go-related gene channel trafficking. J Pharmacol Exp Ther 320: 525–534.

Zhang YH, Cheng H, Alexeenko VA, Dempsey CE, Hancox JC (2010). Characterization of recombinant hERG K(+) channel inhibition by the active metabolite of amiodarone desethyl-amiodarone. J Electrocardiol 43: 440–448.

Zitron E, Kiesecker C, Scholz EP, Lück S, Bloehs R, Kathöfer S *et al*. (2004). Inhibition of cardiac HERG potassium channels by the atypical antidepressant trazodone. Naunyn Schmiedebergs Arch Pharmakol 370: 146–156.